Effect of dc bias on the Curie–Weiss exponent in 0.76Pb(Mg$_{1/3}$Nb$_{2/3}$)O$_3$−0.24PbTiO$_3$ ferroelectric single crystal

S. G. Lu,[a] Z. K. Xu,[b] and Haydn Chen
Department of Physics and Materials Science, City University of Hong Kong, Tat Chee Avenue, Kowloon, Hong Kong, China

X. Y. Zhao and H. S. Luo
The State Key Laboratory of High Performance Ceramics and Superfine Microstructure, Shanghai Institute of Ceramics, Chinese Academy of Sciences, 215 Chengbei Road, Jiading, Shanghai 201800, China

J. Wang, H. L. W. Chan, and C. L. Choy
Department of Applied Physics and Materials Research Centre, The Hong Kong Polytechnic University, Hung Hom, Kowloon, Hong Kong, China

Permittivity versus temperature characteristics and Curie–Weiss exponent (CWE) γ in the universal Curie–Weiss law $[\varepsilon^{-1}=\varepsilon_m^{-1}[1+(T-T_c)^\gamma/(2\delta^2)]](1\leqslant\gamma\leqslant2)]$ as a function of dc bias field were obtained for ⟨001⟩, ⟨011⟩, and ⟨111⟩ oriented 0.76Pb(Mg$_{1/3}$Nb$_{2/3}$)O$_3$−0.24PbTiO$_3$ single crystals. Results indicated that γ is a function of dc bias field and three different oriented crystals show slight different γ values but the similar dc field dependence. © *2005 American Institute of Physics.* [DOI: 10.1063/1.1897063]

Relaxor ferroelectric (RF) Pb(Mg$_{1/3}$Nb$_{2/3}$)O$_3$−PbTiO$_3$ (PMN-PT) single crystals near the morphotropic phase boundary (MPB) have attracted considerable attention due to their outstanding dielectric, piezoelectric, and electro-optic properties.[1,2] Recently, their microstructure and phase transition behavior as a function of direct current (dc) bias field (E_{dc}) have been intensively investigated by x-ray diffraction (XRD), neutron scattering, optical microscopy (OM), transmission electron microscopy (TEM), and scanning force microscopy (SFM).[3–5] The structural characterizations visualize the correlation between the microstructure and the macroscopic properties of the relaxor ferroelectric crystals under a dc bias field. Investigations have also demonstrated that the external dc bias field can strongly affect the permittivity by influencing the electric domain, phase transition, and the peak temperature of maximum permittivity T_{max}.[3–6] It is crucial to understand the effect of dc bias field on permittivity if the materials are used as tunable dielectrics for radio frequency and microwave devices.

For ferroelectric (FE) materials, either normal or relaxor ferroelectrics, the universal Curie–Weiss law can be written as[7,8]

$$\varepsilon^{-1} = \varepsilon_m^{-1}[1 + (T - T_{max})^\gamma/(2\delta^2)](1\leqslant\gamma\leqslant2), \qquad (1)$$

where, ε is permittivity, ε_m is maximum permittivity, T is temperature, T_{max} the peak temperature of maximum permittivity, δ is a distribution parameter of the degree of the dielectric relaxation over a temperature region, γ the Curie–Weiss exponent (CWE). Usually, for normal ferroelectrics, $\gamma=1$; while for relaxor ferroelectrics, $\gamma=2$.[8] Any other γ value between 1 and 2 is an indication of relative amount of RF and FE presented in a ferroelectric. Although γ is mainly associated with the paraelectric phase (PE) above T_{max}, it contains the information of ferroelectric performance of materials. In addition, it should be noticed that for relaxor fer-

roelectrics, nanometer sized domains play a critical role in resulting in observed dielectric anomaly. The existence of nanometer sized region, or so called Kanzig region,[9] has smeared the boundary between the FE-PE phases over a wide temperature range. It is possible to use the universal Curie–Weiss law to analyze the permittivity and associated change in domain structure over a wide temperature range above T_{max}.

In this work, the permittivity as a function of temperature and dc bias field was measured and fitted using the universal Curie–Weiss law [Eq. (1)], the γ values were obtained and discussed in terms of the permittivity–temperature characteristics. The fitting was carried out using the nonlinear curve fitting method in the Microcal Origin (Version 6.0, Microcal Software, Inc.). During the fitting, the T_{max} was fixed, the other three parameters (ε_m, δ, and γ) were altered to get optimized values. Then the Curie–Weiss exponent γ can be obtained.

The 0.76PMN-0.24PT single crystal was grown using a modified Bridgman method. After the growth, the crystal was cut into small pieces with a size of $5\times5\times1$ mm^3 and three orientations along ⟨001⟩, ⟨011⟩, and ⟨111⟩, respectively. Before electrical measurement, silver paste was coated on both surfaces of the crystals and annealed at 650 °C for 15 min to form an Ohmic contact. The electrical measurement was carried out using a multifrequency inductance-capacitance-resistance (LCR) Meter (Model SR720, Stanford Research Systems) at 1 kHz, temperature ranging from 20 to 250 °C, with a heating rate 1 °C/min, and dc bias field ranging from 0 to 300 kV/m. Before measurement, the crystal was thermally depoled at 240 °C.

The permittivity as a function of temperature and E_{dc} are sketched in Figs. 1–3, for ⟨001⟩, ⟨011⟩, and ⟨111⟩ oriented PMN-PT crystals, respectively. For ⟨001⟩ oriented crystal (see Fig. 1), when increasing the E_{dc} to 100 kV/m, T_d appears, at which the domains change from micro-sized to nano-sized ones.[10] When further increasing the E_{dc}, T_d, and T_{max} shifts toward high temperatures. At T_{max}, there is a

---

[a]Electronic mail: apsglu@cityu.edu.hk
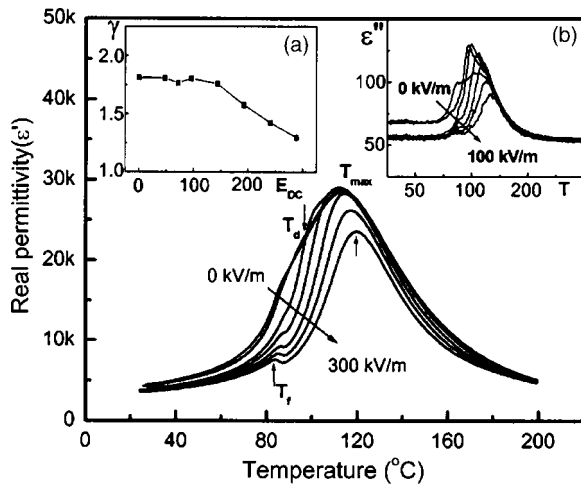[b]Electronic mail: apzkx@cityu.edu.hk

86, 142905-1

FIG. 1. Permittivity as a function of temperature and dc bias field for $\langle 001 \rangle$ oriented 0.76PMN-0.24PT crystal at 1 kHz. Inset (a) is the γ as a function of dc bias field. Inset (b) is the imaginary part of permittivity. T_d, T_f, and T_{max} are indicated with arrows.

FIG. 3. Permittivity as a function of temperature and dc bias field for $\langle 111 \rangle$ oriented 0.76PMN-0.24PT crystal at 1 kHz. Inset (a) is the γ as a function of dc bias field. Inset (b) is the imaginary part of permittivity. T_d and T_{max} are indicated with arrows.

transformation from RF to PE phase. At 150 kV/m, a small peak near 83 °C appears, it is associated with the transition from rhombohedral to tetragonal phase,[11] the transition temperature is specified as T_f. This peak becomes sharper, and shifts toward low temperatures with further increasing E_{dc}. The imaginary part of permittivity [ε'', inset (b) of Fig. 1] demonstrates two peaks, one weak peak is micro-sized to nano-sized domain change, the other strong peak is RF–PE transition, which shifts toward high temperature with increasing E_{dc}.

The γ as a function of E_{dc} is shown in the inset (a). The γ does not significantly change when $E_{dc} < 100$ kV/m, which means that the weak external dc bias field does not significantly change the randomly oriented nanometer sized domains. When further increasing the E_{dc} to 150 kV/m, a micron sized tetragonal phase starts to appear, and micron sized domains align along the E_{dc} together with the nanometer sized domains,[11] then the γ decreases monotonously with further increasing E_{dc} due to increased domain size.

For $\langle 011 \rangle$ oriented crystal, similar to $\langle 001 \rangle$ oriented one, a T_d (~ 84 °C) also appeared when a E_{dc} was applied to the
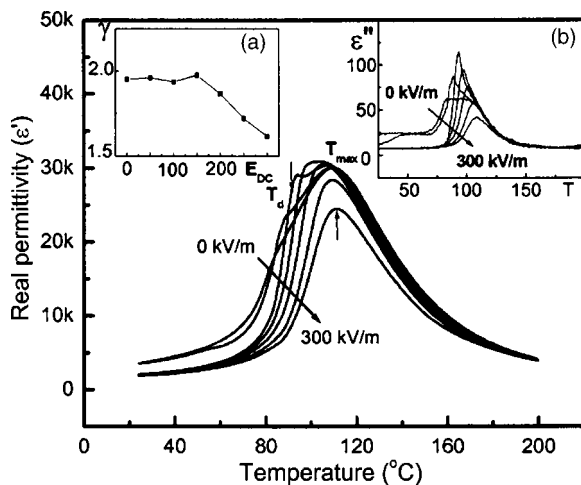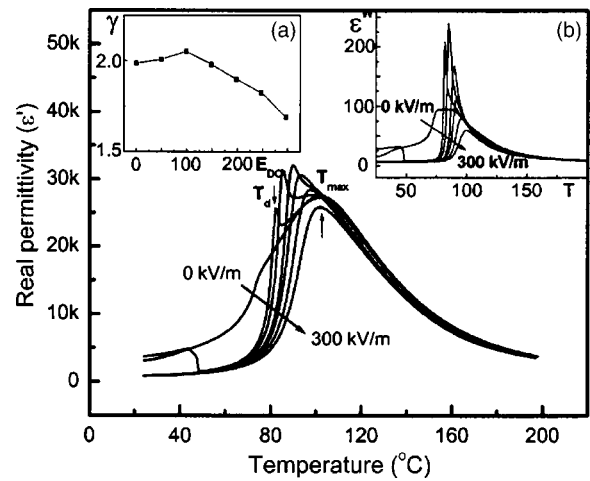

FIG. 2. Permittivity as a function of temperature and dc bias field for $\langle 011 \rangle$ oriented 0.76PMN-0.24PT crystal at 1 kHz. Inset (a) is the γ as a function of dc bias field. Inset (b) is the imaginary part of permittivity. T_d and T_{max} are indicated with arrows.

crystal (see Fig. 2). The γ versus E_{dc} is plotted in the inset (a) of Fig. 2. When increasing the E_{dc} to 100 kV/m, T_d moves to ~ 90 °C, indicating the temperature at which field-induced domain changes from micro-size to nano-size shifts toward high temperature. The γ does not significantly change with the E_{dc} when $E_{dc} < 150$ kV/m. When further increasing the E_{dc} to above 150 kV/m, T_d approaches T_{max}, and more and more nanometer sized domains align along the E_{dc}. Then peak permittivity ε_m decreases, and the γ decreases as well because the randomness of the orientation of nanometer sized domains decreases. And T_{max} shifts toward high temperatures because the E_{dc} stabilizes the ferroelectric phase.[6] The imaginary part of permittivity [ε'', inset (b) of Fig. 2] demonstrates the same features as those in $\langle 001 \rangle$ oriented crystal.

For the $\langle 111 \rangle$ oriented crystal (see Fig. 3), when $E_{dc} = 50$ kV/m, a peak appears at 44 °C. The origin of this peak is still under investigation. It is found that the T_d appears at 83 °C and shifts toward high temperatures with increasing E_{dc}. It is interesting to note that differing from $\langle 001 \rangle$ and $\langle 011 \rangle$ oriented crystals, a peak near T_d shifts close to the T_{max} peak and is higher than the T_{max} peak with increasing E_{dc}. The γ as a function of E_{dc} is shown in the inset (a) of Fig. 3. It has been verified that 150 kV/m is the coercive electric field of 0.76PMN-0.24PT poled along the $\langle 111 \rangle$ direction at 80 °C.[11] When further increasing the E_{dc} to over the coercive field, T_{max} shifts toward high temperature, more domains align along the field, and the γ thus decreases. The imaginary part of permittivity [ε'', inset (b) of Fig. 3] demonstrates the same features as those in the $\langle 001 \rangle$ oriented crystal. The difference is that the micro-sized to nano-sized domain change instead of RF-PE transition, is very sharp, consistent with the sharp peaks of real parts (ε') near T_d.

The γ values slightly differ for three oriented PMN-PT crystals. All of them decrease with increasing E_{dc} when $E_{dc} > 150$ kV/m. For $\langle 001 \rangle$, $\langle 011 \rangle$, and $\langle 111 \rangle$ oriented crystals, γ values change from 1.81 to 1.29, 1.96 to 1.61, and 2.05 to 1.68, respectively, when E_{dc} increases from 0 to 300 kV/m. Three different oriented crystals show slight different γ values but the similar dc field dependence. The origin of this difference is to be answered.

On the other hand, the coercive electrical field E_c has a significant impact on the γ in terms of the domain alignment. When the E_{dc} is less than E_c, the permittivity decreases slightly, and γ does not significantly change with E_{dc}. When $E_{dc} > E_c$, the permittivity reduces considerably, then γ monotonously decreases with E_{dc}. It is especially obvious when the E_{dc} is applied along the polar direction $\langle 111 \rangle$.

As for the γ itself, γ is a reflection of compositional fluctuation,[12] nano-domain,[13] nanocluster,[14] nano-sized inhomogeneity or random field,[15,16] etc. Under an external dc bias field, the γ decreases with increasing E_{dc}. Very recently, electric field driven tunable properties have been reported in $(BaSr)TiO_3$ (BST), $Ba(SnTi)O_3$ (BSnT),[17] and $Ba(ZrTi)O_3$ (BZT),[18] etc. Accordingly their γ values are expected to remarkably change with E_{dc}. One can use γ to quantitatively assess the effect of external dc bias field on the permittivity–temperature characteristics.

In summary, the permittivity as a function of temperature and dc bias field for 0.76PMN-0.24PT relaxor ferroelectric single crystals was measured. Universal Curie–Weiss law was used to fit the field biased permittivity–temperature characteristics. It was found that γ did not significantly change with the field when $E_{dc} < E_c$, but monotonously decreased with E_{dc} when $E_{dc} > E_c$. For $\langle 001 \rangle$, $\langle 011 \rangle$, and $\langle 111 \rangle$ oriented crystals, γ values change from 1.81 to 1.29, 1.96 to 1.61, and 2.05 to 1.68, respectively when E_{dc} increases from 0 to 300 kV/m. Three different oriented crystals show slight different γ values but the similar dc field dependence.

[1]S. W. Choi, T. R. Shrout, S. J. Jang, and A. S. Bhalla, Ferroelectrics **100**, 29 (1989).
[2]R. E. Service, Science **275**, 1878 (1997).
[3]F. M. Bai, N. G. Wang, J. F. Li, D. Viehland, P. M. Gehring, G. Y. Xu, and G. Shirane, J. Appl. Phys. **96**, 1620 (2004).
[4]Z.-G. Ye, B. Noheda, M. Dong, D. Cox, and G. Shirane, Phys. Rev. B **64**, 184114 (2001).
[5]A. K. Singh and D. Pandey, Phys. Rev. B **67**, 064102 (2003).
[6]M. E. Lines and A. M. Glass, *Principle and Application of Ferroelectrics and Related Materials* (Oxford University Press, New York, 1977), p. 169.
[7]H. T. Martirena and J. C. Burfoot, Ferroelectrics **7**, 151 (1974).
[8]Z.-Y. Cheng, L. Y. Zhang, and X. Yao, J. Appl. Phys. **79**, 8615 (1996).
[9]G. A. Smolensky, J. Phys. Soc. Jpn. **28**, Suppl. 26 (1970).
[10]G. S. Xu, H. S. Luo, P. C. Wang, Z. Y. Qi, and Z. W. Yin, Chin. Sci. Bull. **45**, 1380 (2000).
[11]X. Y. Zhao, J. Wang, Z. Peng, H. L. W. Chan, C. L. Choy, and H. S. Luo, Mater. Res. Bull. **39**, 223 (2004).
[12]A. E. Glazounov and A. K. Tagantsev, Phys. Rev. Lett. **85**, 2192 (2000).
[13]L. E. Cross, Ferroelectrics **76**, 241 (1987).
[14]W. Kleemann, P. Licinio, Th. Woike, and R. Pankrath, Phys. Rev. Lett. **86**, 6014 (2001).
[15]V. Bobnar, Z. Kutnjak, R. Pirc, R. Blinc, and A. Levstik, Phys. Rev. Lett. **84**, 5892 (2000).
[16]S. J. Zhang, S. Priya, E. Furman, T. R. Shrout, and C. A. Randall, J. Appl. Phys. **91**, 6002 (2002).
[17]S. G. Lu, Z. K. Xu, and Haydn Chen, Appl. Phys. Lett. **85**, 5319 (2004).
[18]Zhi Yu, Chen Ang, R. Y. Guo, and A. S. Bhalla, Appl. Phys. Lett. **81**, 1285 (2002).